Modifications of critical heat flux models on horizontal surfaces in pool boiling using interfacial instabilities of viscous potential flows

Jong Hyuk Lee, Byoung Jae Kim, and Kyung Doo Kim
Korea Atomic Energy Research Institute(KAERI), 111, Daedeok-daero 989, Yuseong-gu, Daejeon, 305-353, Republic of Korea
leejonghyuk@kaeri.re.kr; byoungjae@kaeri.re.kr; kdkim@kaeri.re.kr

ABSTRACT

Interfacial instabilities play an important role in the development of critical heat flux (CHF) models. The Rayleigh-Taylor, Kelvin-Helmholtz, and Plateau-Rayleigh instabilities are used to formulate the critical heat flux models for saturated pool boiling on infinite horizontal surfaces. The most of existing CHF models have been developed with the results of the linear stability analysis of inviscid flows. Therefore, there is no consideration on the effect of fluid viscosities in the existing CHF models. In fact, as the pressure increases, the viscosities of vapor and liquid become closer. And thus the effect of fluid viscosities cannot be ignored. In this study, we applied the interfacial instabilities of viscous potential fluids including the effect of fluid viscosities on CHF. The viscous potential flow allows a velocity discontinuity at the interface but consider the viscous normal pressure on the interface. These treatments are consistent with the phenomena that the interface waves are induced by pressure, more than by shear force. The circular jet and Kelvin-Helmholtz instabilities of viscous potential flows were applied to the most widely used models: the hydrodynamic theory model. The CHF models were successfully modified to include the effect of fluid viscosities by the interfacial instability analysis of viscous potential flow. The modified models showed better predictions in the wide range of pressure. The reason is attributed to the inclusion of the effect of fluid viscosities considering the critical relative velocity between gas and liquid.

KEYWORDS
Critical Heat Flux (CHF), Viscous potential flow, Interfacial instability, Pool boiling

1. INTRODUCTION

Accurate prediction of critical heat flux(CHF) is very important in nuclear reactor design and safety analysis. Because a CHF can be the upper limit of efficient cooling condition and safety. A number of studies on CHF have been conducted analytically and experimentally [1-3]. However, the CHF prediction theories and mechanisms have not yet been established clearly. Likewise, we noticed that the effect of fluid viscosities is not considered in the most of existing models for saturated pool boiling on infinite horizontal surfaces. The hydrodynamic theory was widely used to introduce the CHF models. However, it has been developed by depending on the Rayleigh-Taylor, Kelvin-Helmholtz, and Plateau-Rayleigh instabilities for inviscid fluids. It is required to consider the effect of viscosity on the instabilities to explain the CHF phenomena more physically. Especially, the effect of gas viscosity on the instabilities cannot be neglected as the radius or thickness of the gas layer is thin. And, all instabilities cannot be neglected as viscosities between gas and liquid become closer.

Recently, Kim et al[4] showed that the Rayleigh-Taylor instability should be analyzed with a thin layer of viscous gas instead of a thick layer of inviscid gas for the model development of critical heat flux and minimum film boiling. The decrease of the most unstable wavelength, which caused by the consideration

of the effect of viscosity, was shown to improve the prediction accuracy of critical heat flux models for various fluids, particularly at high pressures.

Kim et al[4] dealt with only the most unstable wavelength. We can notice that the existing critical heat flux models still consider the Kelvin-Helmholtz instability of inviscid flows, which affect the maximum vapor escape velocity[5] and the initial liquid macrolayer thickness[6]. Therefore, there is room for improving the prediction accuracy by the help of the Kelvin-Helmholtz instability of viscous fluids. The Kelvin-Helmholtz instability arises when different fluid layers are in relative motion. Usually, a uniform flow is considered in each fluid layer, allowing a velocity discontinuity at the interface, and thus a potential flow of inviscid fluids is analyzed. However, if the viscosity effect is taken into consideration, a non-uniform flow occurs due to the shear stress at the interface. The idea to incorporate the effects of fluid viscosities with the Kelvin-Helmholtz instability can be found in the viscous potential flow theory.

Funada and Joseph[7] studied a viscous potential flow analysis of Kelvin-Helmholtz instability. And, they considered the capillary instability and carried out a stability analysis of a circular jet into another fluid[8, 9]. A viscous potential flow analysis is more accurate than an inviscid flow analysis in terms of the growth rate. Therefore, the critical condition of the Kelvin-Helmholtz instability can be predicted more accurately.

In this study, the interfacial instabilities of viscous potential flows are applied to CHF models for saturated pool boiling on infinite horizontal surfaces, with the aim of including the effects of fluid viscosities. The critical conditions of circular jet and Kelvin-Helmholtz instabilities are incorporated into the hydrodynamic theory model. And, the modified models will be validated by comparing the experimental results with various working fluids.

2. CHF model based on viscous potential flow

2.1. Kelvin-Helmholtz and circular jet instability

Funada and Joseph[7] studied the Kelvin-Helmholtz instability in a stratified flow in which a lighter fluid overlies a heavier fluid in a gravitational field as shown in Fig. 1. If the gas velocity is higher than the liquid velocity, the critical relative velocity, U_c (= U_g-U_f) for the inviscid and viscous potential flow can be given by Eq. (1) and Eq. (2) with no consideration of gravity effect, respectively.

$$U_c^2 = \left[\frac{\tanh(k_c\delta_g)}{\rho_g} + \frac{\tanh(k_c\delta_f)}{\rho_f} \right] \sigma k_c \qquad \text{(inviscid potential flow)} \qquad (1)$$

$$U_c^2 = \frac{\sigma k_c \left[\mu_g \coth(k_c\delta_g) + \mu_f \coth(k_c\delta_f) \right]^2}{\rho_g \mu_f^2 \coth(k_c\delta_g)\coth^2(k_c\delta_f) + \rho_f \mu_g^2 \coth(k_c\delta_f)\coth^2(k_c\delta_g)} \qquad \text{(viscous potential flow)} \qquad (2)$$

where ρ, μ, δ, and k_c are the density, viscosity, layer thickness, and the critical wave number, respectively. And, subscript g and f are the gas phase and liquid phase.

Funada and his co-workers[8] conducted a stability analysis for a circular fluid jet into another fluid (Fig.1b). Capillary and Kelvin-Helmholtz instabilities governed the instability phenomena for the circular jet. If the relative jet velocity compared to surrounding fluid velocity is zero, the capillary instability is dominant in this condition. On the other hands, the Kelvin-Helmholtz instability is more dominant, as the relative jet velocity increases. In this study, the only case for a gas jet into liquid is considered. Then the critical relative velocities for inviscid and viscous potential flow are given as follows

$$U_c^2 = \frac{\sigma(\alpha_g \rho_g + \alpha_f \rho_f)}{\alpha_g \alpha_f \rho_g \rho_f}\left(k_c - \frac{1}{R^2 k_c}\right) \quad \text{(inviscid potential flow)} \tag{3}$$

$$U_c^2 = \frac{\sigma(\beta_g \mu_g + \beta_f \mu_f)^2}{\alpha_g \rho_g \beta_f^2 \mu_f^2 + \alpha_f \rho_f \beta_g^2 \mu_g^2}\left(k_c - \frac{1}{R^2 k_c}\right) \quad \text{(viscous potential flow)} \tag{4}$$

where R is the diameter of gas jet. The non-dimensional variables α_g, α_f, β_g, and β_f are defined as $\alpha_g = \frac{I_0(Rk_c)}{I_1(Rk_c)}$, $\alpha_f = \frac{K_0(Rk_c)}{K_1(Rk_c)}$, $\beta_g = \alpha_g - \frac{1}{Rk_c}$, and $\beta_f = \alpha_f + \frac{1}{Rk_c}$, respectively. I_0 and I_1 are the modified Bessel functions of the first kind and K_0 and K_1 are the modified Bessel functions of the second kind. As jet diameter is larger, the values of α_g, α_f, β_g, and β_f approach unity. And, Eq. (3) and (4) will be closer to Eq. (1) and (2) with larger δ_g and δ_f. In other words, the instability of a circular jet with a large diameter is equivalent to the Kelvin-Helmholtz instability with large fluid thickness.

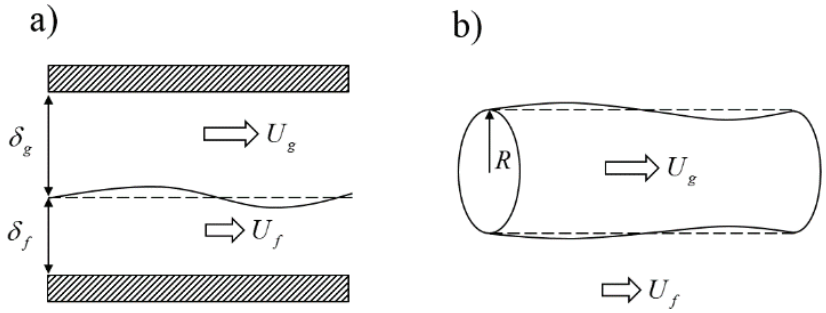

Figure 1. Schematics of a) two fluid flows with different densities in a 2D channel, b) a circular gas jets into a liquid

2.2. Hydrodynamic theory model

The model developed by Zuber[5] was the most widely used to predict the critical heat flux(CHF). Assumed that circular vapor jets rise at the nodes of Taylor waves, the jet diameter has the half value of jet spacing (Fig. 2a). Therefore, the CHF can be formulated in Eq. (5)

$$q_{\max} = \frac{\pi}{16}\rho_g^{1/2} L U_g \tag{5}$$

where U_g is the maximum gas velocity corresponding to the critical condition of the Kelvin-Helmholtz instability. The critical relative velocity for an inviscid flow is

$$U_c = U_g - U_f = \left(\frac{2\pi\sigma}{\lambda_c}\frac{\rho_g + \rho_f}{\rho_g \rho_f}\right)^{1/2} \tag{6}$$

where λ_c is the critical wavelength. In this study, λ_c was the critical wavelength of the capillary waves: $\lambda_c = 2\pi R$, where R is the radius of circular gas jets.

Based on this, Zuber obtained

$$\frac{q_{\max}}{\rho_g^{1/2} L(\sigma \Delta \rho g)^{1/4}} = \frac{\pi}{24}\frac{(16-\pi)\rho_f}{\pi\rho_g + (16-\pi)\rho_f}\left(\frac{\rho_f + \rho_g}{\rho_f}\right)^{1/2} \tag{7}$$

where L is the latent heat. The above equation can be approximated as shown as Eq. (8) at low pressures.

$$\frac{q_{\max}}{\rho_g^{1/2} L(\sigma \Delta \rho g)^{1/4}} = 0.131 \tag{8}$$

However, there is an inconsistency in deriving process of Zuber's model. Although Eq. (7) is the result coming from the Kelvin-Helmholtz instability, λ_c in Eq. (7) uses the critical wavelength of capillary waves. Referring to Eq. (3) and (4), critical relative velocity for circular gas jets is zero because k_c is *1/R*. This means that the vapor velocity and CHF will be zero if in pool boiling.

The Rayleigh-Taylor instability analysis should be used to avoid the non-physical meaning. As with Zuber[5], the radius of circular gas jets assumed $\lambda_d/4$, where λ_d is the most unstable wavelength of Rayleigh-Taylor instability. Using the conservation of mass,

$$U_f = -\frac{\pi}{16-\pi}\frac{\rho_g}{\rho_f} U_g \tag{9}$$

For an inviscid flow, critical velocity for a gas phase can be rewritten using Eq. (3) and (9) as follows.

$$U_g = \frac{(16-\pi)\rho_f}{\pi\rho_g + (16-\pi)\rho_f}\left[\frac{\sigma(\alpha_g\rho_g + \alpha_f\rho_f)}{\alpha_g\alpha_f\rho_g\rho_f}\left(k_c - \frac{16}{\lambda_d^2 k_c}\right)\right]^{1/2} \tag{10}$$

Upon substitution of Eq. (10) into Eq. (6),

$$q_{\max} = \frac{\pi}{16}\left(k_c - \frac{16}{\lambda_d^2 k_c}\right)^{1/2} \frac{(16-\pi)\rho_f}{\pi\rho_g + (16-\pi)\rho_f} \rho_g^{1/2} L\left[\frac{\sigma(\alpha_g\rho_g + \alpha_f\rho_f)}{\alpha_g\alpha_f\rho_f}\right]^{1/2} \tag{11}$$

The most unstable wavelength, λ_d is given by the Rayleigh-Taylor instability. However, there is a drawback of the Rayleigh-Taylor instability for the viscous potential flow. The most unstable wavelength tends to increase unboundedly as the thickness of the gas layer was decreased. Either a fully viscous flow analysis of lubrication approximation should be applied when gas layer is thin[4]. Then λ_d and k_c are given by $2\pi\left(2\sigma/\left(\Delta\rho g\right)\right)^{1/2}$ for a thin layer of gas and $\gamma\left(\Delta\rho g/\sigma\right)^{1/2}$, respectively. We can write Eq. (11) as

$$\frac{q_{\max}}{\rho_g^{1/2} L(\sigma \Delta \rho g)^{1/4}} = \frac{\pi}{16}\left(\gamma - \frac{2}{\pi^2\gamma}\right)^{1/2} \frac{(16-\pi)\rho_f}{\pi\rho_g + (16-\pi)\rho_f}\left[\frac{(\alpha_g\rho_g + \alpha_f\rho_f)}{\alpha_g\alpha_f\rho_f}\right]^{1/2} \tag{12}$$

For large jet diameters, the above equation changes into Eq. (7).

Now, let us consider a viscous potential flow. Eq. (4) is combined with Eq. (9) to give

$$U_g = \frac{(16-\pi)\rho_f}{\pi\rho_g + (16-\pi)\rho_f}\left[\frac{\sigma(\beta_g\mu_g + \beta_f\mu_f)^2}{\alpha_g\rho_g\beta_f^2\mu_f^2 + \alpha_f\rho_f\beta_g^2\mu_g^2}\left(k_c - \frac{16}{\lambda_d^2 k_c}\right)\right]^{1/2} \tag{13}$$

Substituting this into Eq. (5) and using $\lambda_d = 2\pi(2\sigma/(\Delta\rho g))^{1/2}$ and $k_c = \gamma(\Delta\rho g/\sigma)^{1/2}$, we obtain the revised hydrodynamic model based on the viscous potential flow.

$$\frac{q_{\max}}{\rho_g^{1/2} L(\sigma\Delta\rho g)^{1/4}} = \frac{\pi}{16}\left(\gamma - \frac{2}{\pi^2\gamma}\right)^{1/2} \frac{(16-\pi)\rho_f}{\pi\rho_g + (16-\pi)\rho_f} \frac{\rho_g^{1/2}(\beta_g\mu_g + \beta_f\mu_f)}{(\alpha_g\rho_g\beta_f^2\mu_f^2 + \alpha_f\rho_f\beta_g^2\mu_g^2)^{1/2}} \tag{14}$$

Yagov[10] stated that if one considers only the surface tension and body forces, one inevitably obtains an equation similar to Eq. (7) in view of a dimensional analysis. In fact, most of the critical heat flux models only replace the right-hand side of Eq. (7) by values that are functions of the liquid-gas density ratio. However, it is noteworthy that Eq. (14) includes liquid and gas viscosities.

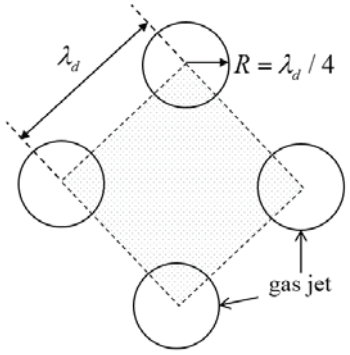

Figure 2. Schematics of pool boiling CHF models using hydrodynamic instability on infinite horizontal surfaces

3. Results and discussion

The obtained equations based on hydrodynamic model contain the only one unknown parameter γ which is coupled with α_g, α_f, β_g, and β_f. Lienhard and Dhir[11] noted that Eq. (7) slightly underpredicts compared to the experimental data of various liquids. They modified the equation by defining the numerical constant as follows.

$$\frac{q_{\max}}{\rho_g^{1/2} L(\sigma\Delta\rho g)^{1/4}} = 0.149 \frac{(16-\pi)\rho_f}{\pi\rho_g + (16-\pi)\rho_f}\left(\frac{\rho_f + \rho_g}{\rho_f}\right)^{1/2} \tag{15}$$

Using this constant and Eq. (14), the unknown value of γ was numerically estimated for various liquids as shown in Table I. Interestingly, γ does not vary significantly for all fluids, except for water. The averaged values of five liquids except water are used to predict the CHF for those liquids using the modified hydrodynamics model in Eq. (14).

Fig. 3 through Fig. 7 show the comparison of the CHF predicted results for organic liquids with experimental results [3, 12-16]. In these figures, predictions marked as present (VPF, Eq. (14)) and present (IPF, Eq. (12)) corresponding to the modified hydrodynamic model based on viscous potential flow and inviscid potential flow, respectively. Although it is difficult to compare the modified model with experimental result, the tendencies predicted by models was similar to the scattered data, quantitatively.

Table I. Estimated parameters for viscous potential flow analysis based on Eq. (15)

Fluid	γ	α_g	α_f	β_g	β_f
Water	1.640	1.179	0.885	0.904	1.160
Methanol	1.081	1.326	0.839	0.910	1.255
Hexane	1.013	1.361	0.830	0.916	1.275
R113	0.996	1.370	0.828	0.918	1.280
Pentane	1.012	1.361	0.830	0.916	1.275
Ethanol	1.017	1.358	0.831	0.916	1.273
Avg.	**1.01**	**1.36**	**0.83**	**0.91**	**1.27**

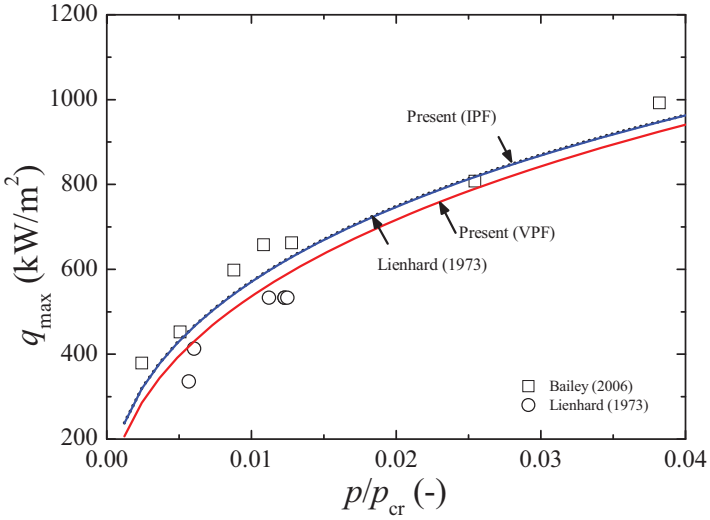

Figure 3. Comparison of the modified models with experimental data for methanol

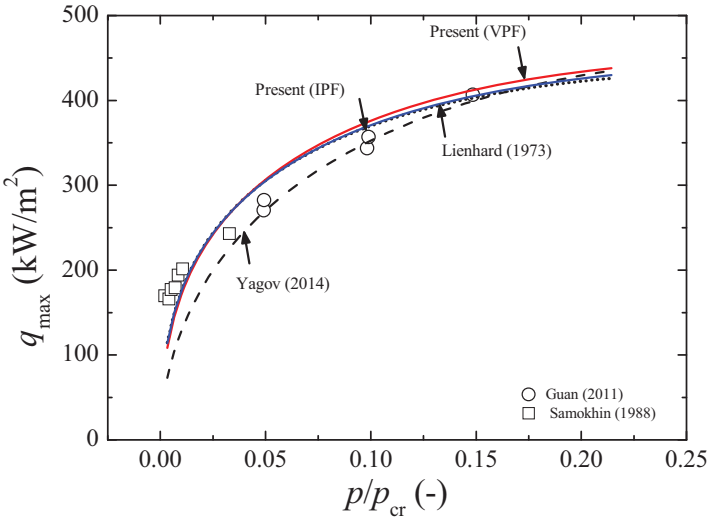

Figure 4. Comparison of the modified models with experimental data for hexane

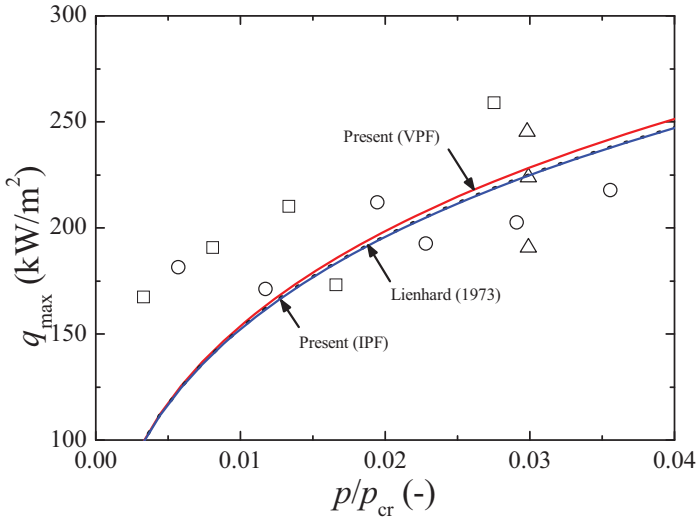

Figure 5. Comparison of the modified models with experimental data for R113

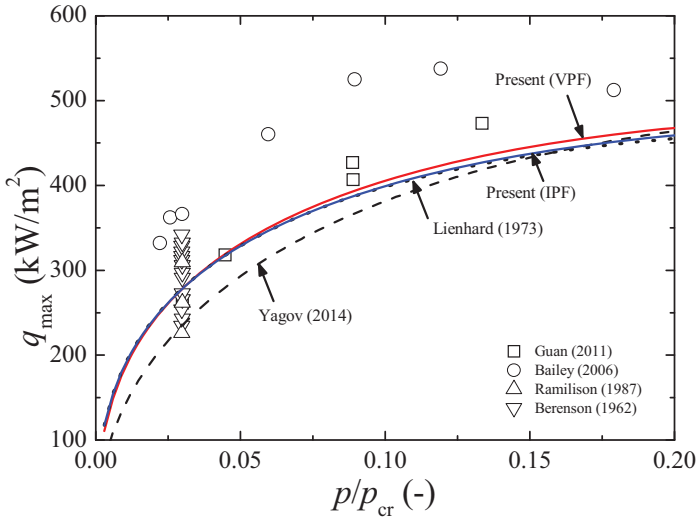

Figure 6. Comparison of the modified models with experimental data for pentane

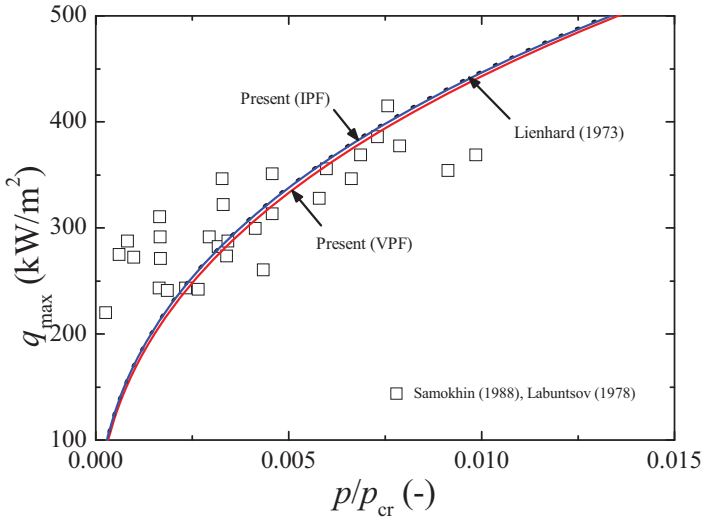

Figure 7. Comparison of the modified models with experimental data for ethanol

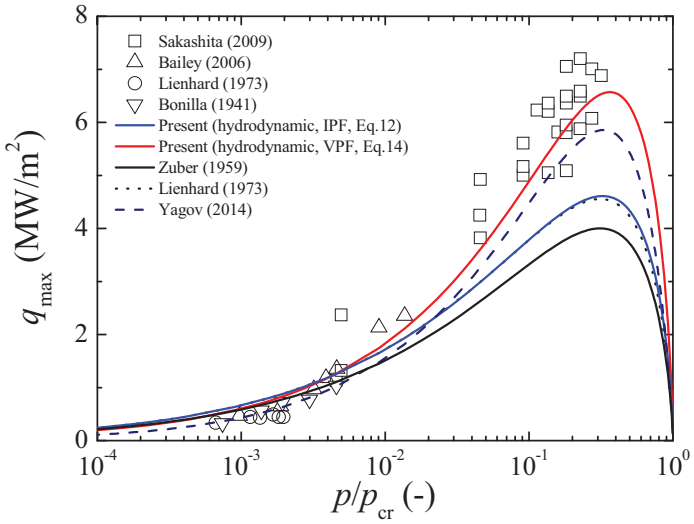

Figure 8. Comparison of the modified models with experimental data for water

Fig. 8 represents the comparison of the predictions between Eq. (12) and (14) with the experimental data of water[10-12, 14, 17]. The models of Zuber(Eq.(7)) [5], Lienhard and Dhir (Eq.(15))[11], and Yagov[10] are also plotted in the figure. There is no difference between the modified model based on inviscid potential flow, Eq. (12), and Lienhard and Dhir's model, Eq. (15). Because it may be attributed that the models are developed based on inviscid potential flows, commonly. However, the modified model based on viscous potential flow shows the improved results at the overall pressure conditions.

Based on all results for organic liquids, the modified model based on viscous potential flow show prediction accuracies similar to the ones based on inviscid potential flow and Lienhard and Dhir [11]. One

of reasons may be attributed to the high viscosity ratios for organic fluids. Fig. 9 shows the ratio of the liquid viscosity to the vapor viscosity according to the various pressure. The effect of viscosity on CHF cannot be neglected as the vapor and liquid viscosities become closer. However, the vapor density for the organic fluids is considerably lower than the liquid one. And thus, the viscosity may not be as effective as expected.

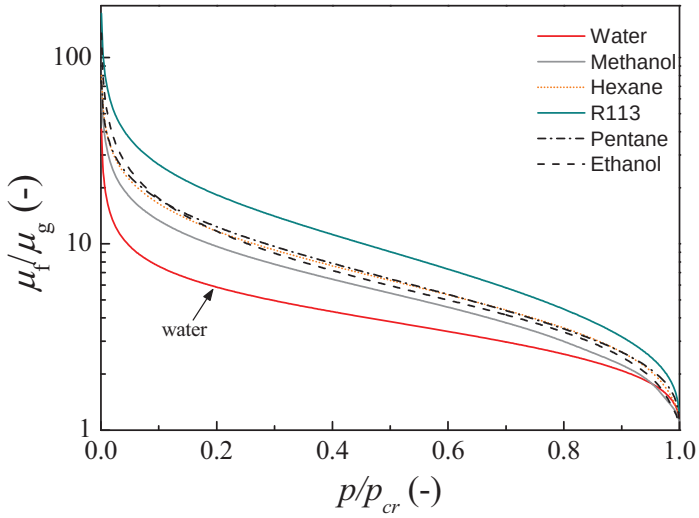

Figure. 11 Variations of the viscosity rations with the changes of pressure

4. CONCLUSIONS

The interfacial instabilities based on the viscous potential theory are incorporated into the most widely used models: the hydrodynamic theory model. The circular jet and Kelvin-Helmholtz instabilities of viscous potential flows are used. The viscous potential flow permits a velocity slip at the interface, but it includes the effect of the viscous normal pressure. These treatments are consistent with the fact that the interface waves are induced more by pressure than by shear force. For water the circular jet instability of a viscous potential flow shows a considerable improvement. For organic liquids, the modified models show prediction accuracies similar to the other original models because it may be swallowed by the higher viscosity ratio. However, we expected that the models become more physically accurate by the including of the effects of fluid viscosities.

NOMENCLATURE

A_g : Total bottom area of vapor stems (m^2)

A_w : Area of the heated surface (m^2)

f : Bubble detachment frequency (1/s)

g : Gravitational acceleration (m/s^2)

k_c : Critical wavelength (1/m)

L : Latent heat (J/kg)

M : $\Delta\rho g\mu_f^4 / (\rho_f^2\sigma^3)$ (Morton number) (−)

$q_{\max}$: Critical heat flux (W/m^2)

R : Diameter of gas jet (m)

U_c : Relative velocity between gas and liquid at the critical condition in which the growth rate is zero (m/s)

U : Fluid velocity (m/s)

Greek symbols

α_g : $I_0(Rk_c) / I_1(Rk_c)$ (−)

α_f : $K_0(Rk_c) / K_1(Rk_c)$ (−)

β_g : $\alpha_g - 1/Rk_c$ (−)

β_f : $\alpha_f + 1/Rk_c$ (−)

γ : $k_c(\Delta\rho g/\sigma)^{-1/2}$ (−)

δ : Thickness of the fluid layer (m)

δ_c : Initial macrolayer thickness (m)

$\Delta\rho$: $\rho_f - \rho_g$ (kg/m^3)

λ_c : Critical wavelength (m)

$\lambda_{c,\text{ipf}}$: Critical wavelength of the Kelvin-Helmholtz instability for inviscid potential flow (m)

$\lambda_{c,\text{vpf}}$: Critical wavelength of the Kelvin-Helmholtz instability for viscous potential flow (m)

λ_d : Most unstable wavelength (m)

η : $\delta_c / \lambda_{c,\text{vpf}}$ (−)

ν : Kinematic viscosity (m^2/s)

μ : Dynamic viscosity (kg/m·s)

ρ : Density (kg/m^3)

σ : Surface tension (N/m)

Subscripts

g : Gas phase

f : Liquid phase

ACKNOWLEDGMENTS

This work was supported by the Nuclear Power Technology Development Program in the form a Korea Institute of Energy Technology Evaluation and Planning (KETEP) grant funded by the Korean Ministry of Knowledge Economy (MKE). This work was supported by the National Research Foundation of Korea (NRF) Grant funded by the Korean Government (MSIP) (no. 2012M2A8A4026028)

REFERENCES

1. V.K. Dhir, "Nucleate and transition boiling heat transfer under pool and external flow conditions," *International Journal of heat and fluid flow*,**12**(4), 290-314 (1991).
2. Y. Katto, "Critical heat flux," *International Journal of Multiphase Flow*,**20**(53-90 (1994).
3. J.H. Lienhard, "Burnout on cylinders," *Journal of heat transfer*,**110**(4b), 1271-1286 (1988).
4. B.J. Kim, J.H. Lee and K.D. Kim, "Rayleigh–Taylor instability for thin viscous gas films: Application to critical heat flux and minimum film boiling," *International Journal of Heat and Mass Transfer*,**80**(150-158 (2015).
5. N. Zuber,"Hydrodynamic aspects of boiling heat transfer (thesis)," California. Univ., Los Angeles; and Ramo-Wooldridge Corp., Los Angeles, (1959).
6. Y. Haramura and Y. Katto, "A new hydrodynamic model of critical heat flux, applicable widely to both pool and forced convection boiling on submerged bodies in saturated liquids," *International Journal of Heat and Mass Transfer*,**26**(3), 389-399 (1983).
7. T. Funada and D.D. Joseph, "Viscous potential flow analysis of Kelvin–Helmholtz instability in a channel," *Journal of Fluid Mechanics*,**445**(263-283 (2001).
8. T. Funada, D.D. Joseph and S. Yamashita, "Stability of a liquid jet into incompressible gases and liquids," *International journal of multiphase flow*,**30**(11), 1279-1310 (2004).
9. T. Funada and D.D. Joseph, "Viscous potential flow analysis of capillary instability," *International journal of multiphase flow*,**28**(9), 1459-1478 (2002).
10. V.V. Yagov, "Is a crisis in pool boiling actually a hydrodynamic phenomenon?," *International Journal of Heat and Mass Transfer*,**73**(265-273 (2014).
11. J.H. Linehard and V.K. Dhir, "Extended hydrodynamic theory of the peak and minimum pool boiling heat fluxes," NASA CR-2270, NASA, USA, (1973).
12. W. Bailey, E. Young, C. Beduz and Y. Yang, "Pool boiling study on candidature of pentane, methanol and water for near room temperature cooling," *Thermal and Thermomechanical Phenomena in Electronics Systems, 2006. ITHERM'06. The Tenth Intersociety Conference on*, pp. 599-603 (2006).
13. R.F. Gaertner and J.W. Westwater, "Population of active sites in nucleate boiling heat transfer," *Chemical Engineering Progress Symposium Series*,**56**((1960).

14. H. Sakashita and A. Ono, "Boiling behaviors and critical heat flux on a horizontal plate in saturated pool boiling of water at high pressures," *International Journal of Heat and Mass Transfer*,**52**(3), 744-750 (2009).
15. G.I. Samokhin and V.V. Yagov, "Heat transfer and critical heat fluxes with liquids boiling in the region of low reduced pressures," *Thermal Engineering*,**35**(2), 746-752 (1988).
16. L.S. Sterman and J. Korychanek, "Critical heat fluxes during boiling of high-boiling heat carriers," *Atomic Energy*,**29**(5), 1124-1125 (1970).
17. C.F. Bonilla and C.W. Perry, "Heat transmission to boiling binary liquid mixtures," *Chemical Engineering Progresses Symposium Series*, pp. 685-705 (1941).